https://doi.org/10.2352/AIT.2026.1.1.3

From Actuation to Droplet: Fully Coupled Simulations of Inkjet Printhead Dynamics

Vinh-Tan Nguyen and Jason Leong, Institute of High Performance Computing (IHPC), Agency for Science, Technology and Research (A*STAR) (Singapore); Satoshi Watanabe, Seiko Future Creation Inc. (Japan); and Toshimitsu Morooka, SII Printek Inc. (Japan).

Abstract

The generation of ink droplets in piezoelectric drop-on-demand printheads is governed by a tightly coupled multiphysics process involving electromechanical actuation, fluid dynamics, and free surface interactions. Conventional simulation approaches often treat these subsystems separately, thus limiting predictive fidelity for design optimisation. In this study, we introduce a framework for simulating the interaction between the deforming piezoelectric actuator and the ink within the inkchannel. The approach couples a structural model that accounts for piezoelectric behaviour with a compressible, multiphase computational fluid dynamics (CFD) solver. These two solvers are coupled through a partitioned fluid–structure interaction (FSI) approach that enforces strong coupling at the shared interface, allowing the model to reproduce the interaction between the actuator motion and fluid response during droplet generation. The modelling tools are applied to a single inkchannel representative of an industrial recirculating printhead, where a volume-of-fluid (VOF) approach is used to track the evolving ink—air interface. Comparisons with structural and fluid observations for the Seiko RC1536 architecture show that the simulations capture the essential features of jet formation, including the effects of waveform shape, inkchannel configuration, and surface tension. By combining the detailed electromechanical and fluid physics, the proposed framework provides a more predictive basis for analysing and improving inkjet printhead performance. It also offers a foundation for future efforts aimed at refining device geometry, adjusting actuation strategies, and supporting the development of next-generation industrial and functional printing systems.

Introduction

Piezoelectric drop-on-demand (DOD) inkjet printing produces droplets by actively changing the inkchannel volume using piezoelectric actuation. A voltage pulse applied to the piezoelectric walls deforms the channel, generating pressure waves that drive the ejection of a droplet through the nozzle [1]. The characteristics of the emitted droplet—its volume, velocity and stability—are therefore highly sensitive to the temporal shape and magnitude of the actuation waveform.

Industrial printheads have advanced considerably beyond the simplified channel geometries for which classical lumped-element or one-dimensional acoustic models were originally conceived. Modern architectures such as the Seiko RC1536 employ a fully recirculating ink path, an isolated channel structure (ICS) to suppress cross-talk, and shear mode piezoelectric actuation, resulting in a tightly coupled interaction between actuator deformation, internal multiphase flow, and meniscus dynamics at the nozzle [2]. Experimental studies on the RC1536 demonstrate that drop velocity, drop volume, refill behaviour, and allowable throw distance vary strongly with the transient interplay between acoustic pressure waves, chamber compliance and flow-induced interface motion. The ability of such printheads to operate across wide viscosity ranges (8–25 cP) and handle larger pigment sizes further illustrates the need for modelling strategies that capture the full multiphysics behaviour of the jetting process.

Despite these developments, numerical studies of piezoelectric inkjet systems remain dominated by decoupled formulations. Many structural analyses compute piezoelectric deformation in isolation, neglecting realistic fluid loading, whereas fluid dynamics simulations often prescribe idealised wall motions or simplified forcing. Existing three-dimensional CFD studies typically omit compressibility, true piezoelectric electromechanics, free surface motion or recirculating flow architectures. Consequently, essential mechanisms such as actuator–fluid feedback, wave propagation in complex chambers, and the influence of ICS designs on cross-talk are not fully resolved in current modelling frameworks.

To overcome these challenges, we introduce a three-dimensional fluid structure interaction (FSI) methodology that embeds the piezoelectric response directly within the structural solver. Extending our earlier work, the proposed framework couples a finite element piezoelectric actuator model with a compressible, multiphase volume-of-fluid (VOF) solver using a strongly coupled partitioned approach. This enables self-consistent prediction of actuator-driven pressure waves, chamber deformation, ink recirculation, meniscus evolution and droplet formation. The framework provides a high-fidelity tool for analysing waveform design, geometric modifications and operational conditions in next-generation industrial inkjet printheads.

Three-dimensional coupled piezoelectric structure fluid model of inkchannel

This work focuses on a class of recirculating industrial printheads produced by SII Printek Inc. [3]. These devices employ a dedicated recirculation chamber and an isolated channel nozzle arrangement, allowing stable jetting performance across a broad range of inks and substrates. A representative three-dimensional rendering of the RC1536 channel layout is shown in Fig. 2, illustrating how the ink is guided through the chamber while droplet formation is actuated by deformable piezoelectric walls.

The piezoelectric jetting mechanism is a strongly coupled multiphysics process. Applying an electric potential across the actuator induces a deformation of the poled piezoelectic layer. This alters the inkchannel volume and generates acoustic waves within the ink. The resulting unsteady flow then interacts with the inkchannel structure and ultimately results in the formation of a droplet at the nozzle. Capturing this phenomenon requires two numerical models: (i) an electromechanical model capable of resolving the piezoelectric actuator response under an applied voltage, and (ii) a fluid dynamics model that describes the transient ink dynamics and free surface motion during ejection. These models exchange information through the deforming wall, leading to a tightly coupled actuation–flow system. A concise description of both components is provided in the following section.

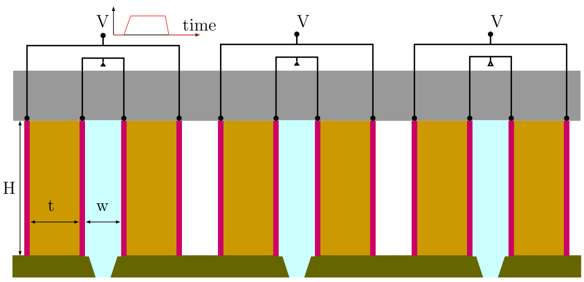

Figure 1. *Schematic of the RC1536 ink channel showing the actuator wall, electrode layout, cover and nozzle plates, and the internal ink chamber. Not to scale.*

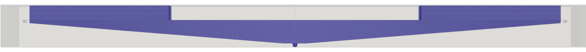

Figure 2. *Three-dimensional rendering of the inkjet head channel geometry, highlighting the piezoelectric actuator region (light grey) and the ink-filled section (dark blue).*

Electromechanical model of the actuator walls

The deformation of the piezoelectric channel walls is governed by the equations of motion for a continuum occupying a domain Ω with boundary $\Gamma = \partial\Omega$. The balance of linear momentum can be written as

$$\rho \ddot{u}_i = \sigma_{ij,j} + \rho f_i^B, \tag{1}$$

while the electric field must satisfy Gauss's law for a charge-free dielectric,

$$D_{i,i} = 0. \tag{2}$$

In these equations, σ_{ij} denotes the components of the Cauchy stress tensor, while D_i represents the electric displacement vector. The quantities ρ and f_i^B correspond to the material density and body force term, respectively. The superscripts and subscripts follow conventional notation: $()_i$ and $()_{ij}$ indicate the ith component of a vector and the (i,j) entry of a second-order tensor. Time and spatial differentiation are expressed using $\ddot{()} = \partial^2()/\partial t^2$ and $()_{,i} = \partial()/\partial x_i$. Gauss's law is written here for a dielectric medium without free charge. The constitutive behaviour of the piezoelectric solid couples the mechanical and electrical fields through

$$\sigma_{ij} = C_{ijkl}\,\varepsilon_{kl} - e_{kij}E_k, \tag{3}$$

$$D_i = e_{ikl}\varepsilon_{kl} + \varepsilon_{ik}E_k, \tag{4}$$

where C_{ijkl}, ε_{ik}, and e_{kij} are the elastic, dielectric, and piezoelectric material constants. The strain tensor is defined by

$$\varepsilon_{kl} = \tfrac{1}{2}(u_{k,l} + u_{l,k}), \tag{5}$$

and, assuming negligible magnetic effects, the electric field follows from the electric potential ϕ as

$$E_i = -\phi_{,i}. \tag{6}$$

The coupled electromechanical governing equations are discretised using a finite element formulation in which both displacement and electrical potential are nodal degrees of freedom. This enables resolution of piezoelectric anisotropy and shear mode coupling that is consistent with standard formulations used for actuator simulations. The specific implementation employed in this work follows the piezoelectric solid model available within the Open-source, Object-Oriented, Finite Element Method (`OOFEM`) framework [4, 5, 6], which was adequate for multi-field structural analysis required in this study. The approach has been previously verified for piezoelectric actuators relevant to inkjet applications [7].

Ink flow model

The ink and surrounding air are represented as an immiscible, compressible two-phase system under isothermal conditions. Their motion is described by the Navier–Stokes equations, which enforce conservation of mass and momentum.

$$\frac{\partial\rho}{\partial t} + \nabla.(\rho\mathbf{u}) = 0, \tag{7}$$

$$\frac{\partial\rho\mathbf{u}}{\partial t} + \rho(\mathbf{u}.\nabla)\mathbf{u} = -\nabla p + \nabla.(\mu\nabla\mathbf{u}) - \mathbf{g}.\mathbf{x}\nabla\rho + \boldsymbol{f}_b. \tag{8}$$

In these equations, ρ denotes the mixture density, p the dynamic pressure, and $\boldsymbol{u}$ the velocity field. The vector $\boldsymbol{g}$ represents gravitational acceleration, while $\boldsymbol{f}_b$ accounts for additional body force contributions acting on the fluid. In this work, the two fluids are modeled as an immiscible mixture using volume-of-fluid approach, in which the indicator function, α represents the volume fraction of the ink phase in a control volume where $\alpha = 1$ means the volume is fully occupied by the ink phase. The interface between two fluids is essentially smeared in the transition from $\alpha = 0$ to $\alpha = 1$. The dynamics of the free surface is modelled as the transport of volume fraction:

$$\frac{\partial\alpha}{\partial t} + \nabla.\mathbf{u}\alpha + \nabla.\mathbf{u_c}\alpha(1-\alpha) = -\frac{\alpha}{\rho}\frac{\mathrm{D}\rho}{\mathrm{D}t} \tag{9}$$

where $\mathbf{u_c}$ is the artificial compression velocity to maintain the sharpness of interface between phases. The mixture properties can be approximated using weighted averaging mean interpolation as

$$\rho = \alpha\rho_1 + (1-\alpha)\rho_2, \tag{10}$$

$$\mu = \alpha\mu_1 + (1-\alpha)\mu_2. \tag{11}$$

In these expressions, the indices 1 and 2 correspond to the ink and air phases, respectively. The interfacial surface tension is incorporated as a volumetric force following the continuous surface force formulation [8], and this contribution is introduced into the momentum equation as an additional body force term:

$$\boldsymbol{f}_b = \boldsymbol{f}_\sigma = \kappa\sigma\nabla\alpha,$$

In this formulation, κ denotes the local interface curvature and σ is the surface tension coefficient. The curvature is obtained directly from the volume fraction field through

$$\kappa = \nabla.\left(\frac{\nabla\alpha}{|\nabla\alpha|}\right). \tag{12}$$

A cell-centred finite volume formulation, as implemented in the `foam-extend` [9] fork of `OpenFOAM` [10], is used to discretise the isothermal, compressible two-phase Navier–Stokes equations.

Fully coupled fluid–piezoelectric–structure interaction model

The interaction between the deforming piezoelectric walls and the surrounding fluid is resolved using a partitioned FSI framework. This strategy enables the solid and fluid domains to be solved by `OOFEM` and `OpenFOAM` respectively while maintaining a consistent exchange of interface quantities. At the fluid–solid boundary, kinematic compatibility is imposed through continuity of displacement, whereas dynamic equilibrium is enforced by matching the tractions transmitted between the two fields. This formulation constitutes a strongly coupled interface condition.

Within the `foam-extend` FSI environment [11], several iterative coupling algorithms are available, including fixed-point (Gauss–Seidel) iterations with either fixed or Aitken Δ^2 relaxation [12], and the interface quasi-Newton approach with inverse Jacobian updates constructed via a least-squares procedure, Interface Quasi-Newton Inverse Least-Squares (IQN–ILS) [13]. These algorithms accelerate convergence by improving the estimate of interface displacements and loads at each iteration.

For each time step, the coupling procedure begins by forming an initial estimate of the interface displacement and evaluating the associated residual. The fluid and solid solvers are then advanced in an alternating manner: face-centred tractions computed on the fluid side are mapped to the solid interface, while nodal displacements from the solid model are transferred back to the fluid mesh, which is subsequently updated through a mesh-motion solution. Both the fluid and solid fields are then resolved using the updated interface information, after which a new interface residual is evaluated. This iterative exchange continues until the interface residual satisfies the prescribed convergence tolerance [14], yielding a fully converged fluid–piezoelectric–structure interaction state for the current time step.

3D coupled FSI simulations of inkjet printheads

The fully coupled FSI framework developed in this work is applied to high-fidelity three-dimensional simulations of an industrial recirculating inkjet printhead. These simulations aim to resolve, within a single unified model, the complete sequence of physical processes governing drop-on-demand jetting: piezoelectric driven wall deformation, the resulting compressible pressure waves in the ink chamber, viscous and inertial flow effects within the nozzle, and the subsequent evolution of the ink–air free surface leading to droplet formation and pinch-off.

By explicitly coupling the electromechanical behaviour of the actuator with the transient multiphase flow field, the model captures the intricate interplay between channel compliance, acoustic wave propagation, and interface dynamics. This enables a physics-based description of jet initiation and droplet ejection that goes beyond simplified or decoupled approaches, providing a predictive tool for analysing waveform sensitivity, geometric effects, and ink property dependence in modern industrial printheads.

The following subsections present the computational setup, coupling strategy, and representative results obtained from the three-dimensional FSI simulations.

Simulation setup and geometry

The three-dimensional simulations are performed on a detailed representation of a single jetting channel from the industrial printhead considered in this study. Only the primary channel is modelled, as the ICS design of the RC1536 printhead ensures that neighbouring channels and the recirculation manifold have negligible influence on the local actuation and droplet formation dynamics. A summary of the channel geometry and the fluid/solid regions incorporated into the model is shown in Fig. 3. The geometric model includes the inkchannel, the piezoelectric actuator wall, the cover and nozzle plates, and the nozzle transition region, enabling the complete actuation–to–ejection process to be captured within a single-channel domain. Key geometric features of the RC1536 architecture are retained to ensure that the predicted flow and deformation fields accurately reflect realistic operating conditions. The computational domain is further reduced by applying two orthogonal symmetry planes, exploiting the ICS of the RC1536 design.

The fluid and solid domains are meshed separately as illustrated in Fig. 3. The structural mesh is discretised with tetrahedral elements while the fluid mesh is constructed using a predominantly hexahedral topology with a uniform cell size of approximately 2 μm in the channel–nozzle region. This mesh resolution is sufficient to resolve the free surface and propagation of acoustic waves in the inkchannel.

The two meshes are generated to be geometrically conformal at the fluid–structure boundary to fascilitate transfer of displacements and tractions during the FSI coupling iterations. This geometric fidelity, together with the mesh resolution in the respective fluid and solid domains provides the foundation for accurately resolving the transient multiphysics phenomena central to inkjet droplet generation.

Inkchannel material properties

The solid components of the printhead are represented using linear elastic constitutive laws. The cover plate and actuator wall are composed of lead–zirconate–titanate (PZT), while the nozzle plate is modelled as an isotropic polyimide layer, consistent with typical industrial printhead assemblies. Only the actuator plates are electromechanically active; the cover plate serves solely as a passive structural layer.

Piezoelectric actuation is implemented using a transversely poled PZT configuration operating in shear mode. In this mode, the applied electric field induces in-plane shear deformation of the actuator wall, governed primarily by the shear mode piezoelectric strain coefficient $d_{15} = 7.80 \times 10^{-12}$ pC/N. All remaining elastic, dielectric, and piezoelectric parameters follow standard values for engineering grade PZT ceramics and polyimide films and are omitted for brevity, as they play a secondary role in the present FSI simulations.

Actuation waveform, boundary conditions, and ink properties

The piezoelectric actuator is driven using a voltage waveform representative of typical industrial operating conditions. In the present study, a unipolar driving pulse with an amplitude of 26 V and a pulse width of 5.5 μs is applied across the oppositely poled Piezo(+) and Piezo(–) layers. This imposed potential difference generates the electric field responsible for the expansion–contraction cycle of the actuator wall. The resulting structural deformation is transferred directly to the fluid domain through the shared fluid–solid interface via the strongly coupled FSI scheme described previously.

To accommodate the wall motion, the interior of the fluid mesh is updated using the `velocityLaplacian` mesh motion method which solves a Laplace equation for the mesh velocity at cell centres, interpolates this velocity to mesh points, and advances the point coordinates using the time-integrated point ve-

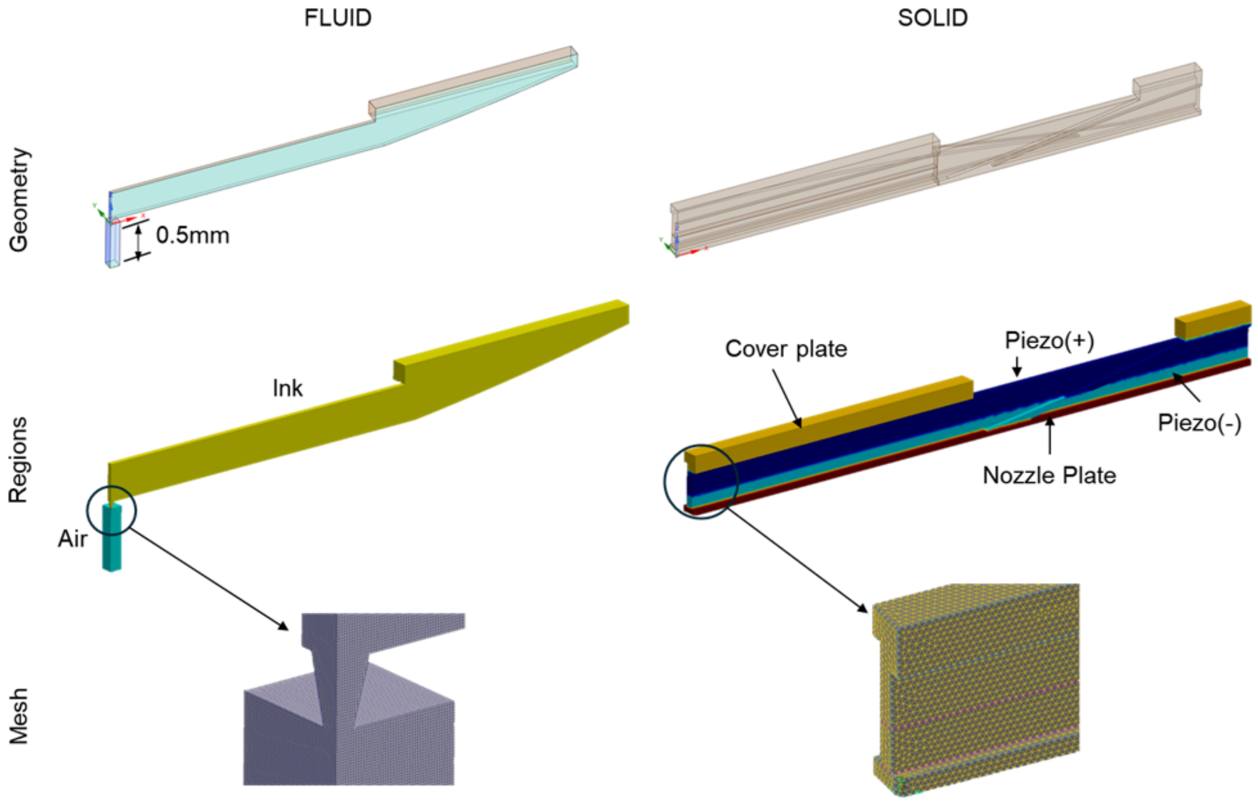

Figure 3. Discretization of the fluid and solid domains. The fluid domain is meshed using predominantly hexahedral cells with a uniform resolution of 2 μm in the inkchannel–nozzle region, resulting in ∼4.7 million cells. The solid domain, comprising the cover plate, nozzle plate, and the piezoelectric actuator assembly, is discretised with ∼190k tetrahedral finite elements. The actuator consists of two piezoelectric plates, labelled Piezo(+) and Piezo(–), which denote oppositely poled layers. The geometry is truncated by two orthogonal symmetry planes. Fluid and solid meshes are constructed to be conformal at the interface.

locities. This formulation has been shown to be robust for the moderate deformations characteristic of inkjet actuation [15].

No-slip boundary conditions are imposed on all solid walls in the fluid domain. The ink–air interface at the nozzle exit is captured implicitly using the volume-of-fluid (VOF) phase fraction field. The outlet employs a Neumann bounday condition, allowing droplets to exit the computational domain without artificial confinement. The fluid and solid domains are truncated by two symmetry planes so that only one quarter of the full simulation volume is resolved.

The ink used in this study is a water-based pigment formulation with material properties and operating parameters summarised in Table 1. These properties influence the acoustic response of the inkchannel, viscous damping, capillary dynamics at the meniscus, and ultimately the droplet formation process.

Table 1. Ink properties and operating conditions.

Application	Textile printing
Ink type	Water-based pigment
Viscosity (mPa·s)	11.20
Surface tension (mN/m)	37.36
Density (g/cm^3)	1.116
Speed of sound (m/s)	1692.52
Temperature (℃)	25
Driving voltage (V)	26
Driving pulse (μs)	5.5
Capillary number (Ca)	1.80
Ohnesorge number (Oh)	0.33

Pressure wave propagation and inkchannel response

The applied voltage pulse induces shear deformation in the piezoelectric actuator wall. Depending on the signal applied, the wall motion can initially increase the inkchannel volume, producing a reduction in chamber pressure. This disturbance generates an acoustic wave that travels through the ink. As it propagates toward the nozzle it encounters geometric features and boundary constraints that give rise to repeated reflections. The superposition of these incident and reflected waves forms the transient pressure field that ultimately controls the motion of the meniscus.

Fig. 5 shows the time evolution of inkchannel pressure and actuator wall displacement. The pressure initially drops as the actuator expands the chamber, followed by a sequence of oscillations associated with acoustic reflections within the confined geometry of the inkchannel. As the oscillations decay, the fluid–structure system relaxes under the combined influence of fluid viscosity and the compliance of the actuator assembly. The wall displacement closely follows the evolving pressure, demonstrating the interaction captured by the coupled FSI approach.

This interaction between the acoustic wave and structural deformation governs the forcing applied to the meniscus. These dynamics set the conditions for interface motion, ligament formation, and ultimately droplet formation. Accurately resolving this behaviour is essential for predicting the full actuation-to-ejection sequence in piezoelectric inkjet systems.

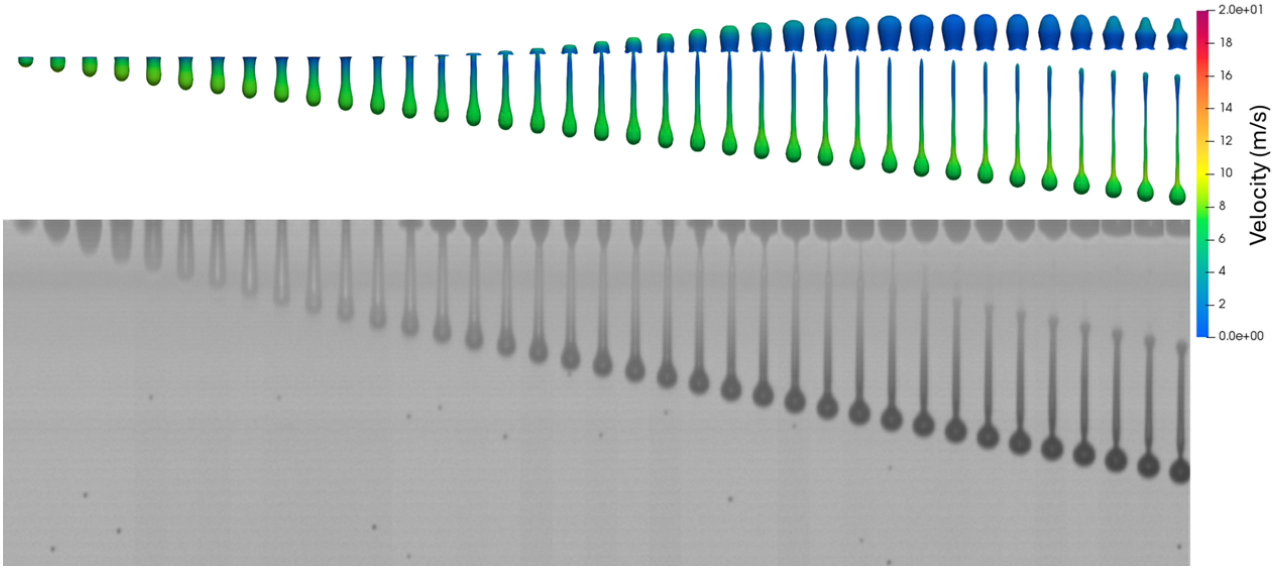

Figure 4. *Actuation-to-ejection droplet formation sequence.* ***Top:*** *Predicted interface evolution and velocity magnitude from the coupled FSI simulation, capturing meniscus deformation, ligament formation, necking and pinch-off.* ***Bottom:*** *Corresponding high-speed jetting images obtained from the printhead under the same operating conditions.*

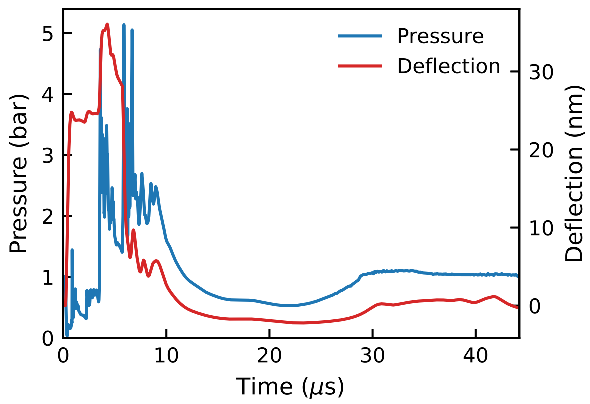

Figure 5. *Inkchannel pressure and actuator wall deflection vs. time predicted by coupled FSI simulation.*

Full actuation-to-ejection simulation

The pressure response described earlier drives the meniscus motion that leads to droplet formation. Once the chamber pressure rises above ambient during the actuation cycle, the meniscus begins to move outward and a ligament forms as ink is accelerated through the nozzle. The subsequent reduction in pressure during the rarefaction stage eventually causes the ligament to detach from the fluid remaining inside the inkchannel. The volume-of-fluid (VOF) formulation tracks the ink–air interface throughout this sequence, capturing the progression from initial meniscus displacement to ligament stretching and final droplet detachment.

Fig. 4 shows a representative ejection sequence predicted by the coupled FSI framework, alongside corresponding high-speed jetting images. The simulation reproduces the characteristic stages observed experimentally: outward meniscus motion, ligament stretching, and formation of the ink droplet. The close qualitative agreement between simulation and experiment demonstrates that the FSI model resolves the key multiphysics mechanisms governing droplet generation in piezoelectric inkjet printing. The solver reproduces realistic jet morphology, breakup behaviour, and droplet kinematics. These results confirm that the proposed FSI framework can capture the complete end-to-end actuation-to-ejection dynamics and provides a solid foundation for future waveform optimisation and design studies.

Conclusion

This work presented a fully coupled three-dimensional fluid–piezoelectric–structure interaction framework for the simulation of piezoelectric drop-on-demand inkjet printheads. The model integrates compressible multiphase flow, piezoelectric actuation, structural dynamics, and mesh motion within a unified finite volume/finite element solution procedure. By resolving the coupled actuation and ejection physics within a single computational domain, the solver captures the complete sequence from voltage-driven wall deformation to pressure-wave propagation, meniscus motion, ligament formation, and final droplet breakup.

High-fidelity simulations of an isolated channel representative of the Seiko RC1536 industrial printhead architecture were performed using experimentally relevant waveforms and ink properties. The predicted chamber pressure response, wall deflection, and droplet formation exhibit strong qualitative agreement with high-speed jetting measurements. The framework successfully reproduces the characteristic features of piezoelectric inkjet operation,including meniscus dynamics, ligament stretching, primary drop formation, and satellite formation behaviour. These results confirm that the coupled FSI formulation provides a physically consistent representation of the multiphysics mechanisms governing droplet generation in industrial printheads.

The solver offers a robust foundation for design exploration and optimisation. Because the complete actuation-to-ejection dynamics are modeled directly, sensitivity to waveform shape, ink rheology, material properties, and geometric features can be examined with high accuracy. Future work will focus on systematic parametric studies, integration of non-Newtonian ink models, refinement of free surface resolution for improved satellite prediction, and development of reduced-order models informed by the high-fidelity FSI simulations. Together, these efforts will enable predictive tools that support next-generation inkjet printhead design and waveform engineering.

Acknowledgments

The authors gratefully acknowledge Masakazu Hirata for project supervision and assistance with jetting photography, and Takayuki Shimizu for contributions to the jetting photography work.

References

[1] Haruhiko Koto. Low voltage ink-jet printhead, October 8 1985. U.S. Patent 4,502,058.

[2] Aliasgar Eranpurwala. Seiko's RC1536 printhead – making jettability wider. In Werner Zapka, editor, *Inkjet Printing in Industry: Materials, Technologies, Systems, and Applications*, chapter 22, pages 555–568. Wiley-VCH, 2022.

[3] RC1536 recirculation series of printheads. https://www.seiko-instruments.de/products/inkjet-print-heads/rc1536-recirculation-inkjet-printhead.html?cHash=9212ca5dbe07a63352da8a21370db323, 2020.

[4] B Patzák and Z Bittnar. Design of object oriented finite element code. *Advances in Engineering Software*, 32(10-11):759–767, October 2001.

[5] B. Patzák. OOFEM - an object-oriented simulation tool for advanced modeling of materials and structures. *Acta Polytechnica*, 52(6):59–66, 2012.

[6] B. Patzák. OOFEM home page. http://www.oofem.org, 2000.

[7] Vinh-Tan Nguyen, Pankaj Kumar, and Jason Leong. Finite element modelling and simulations of piezoelectric actuators responses with uncertainty quantification. *Computation*, 6(4):60, November 2018.

[8] J.U Brackbill, D.B Kothe, and C Zemach. A continuum method for modeling surface tension. *Journal of Computational Physics*, 100(2):335–354, June 1992.

[9] Hrvoje Jasak, Aleksandar Jemcov, and Željko Tuković. OpenFOAM: A C++ library for complex physics simulations. In *Proceedings of International workshop on coupled methods in numerical dynamics*, pages 1–20, 2007.

[10] OpenFOAM home page. https://www.openfoam.org/, 2019.

[11] Extend-Project home page. https://sourceforge.net/projects/foam-extend/, 2018.

[12] Bruce M Irons and Robert C Tuck. A version of the aitken accelerator for computer iteration. *Int. J. Numer. Methods Eng.*, 1(3):275–277, July 1969.

[13] Joris Degroote, Klaus-Jürgen Bathe, and Jan Vierendeels. Performance of a new partitioned procedure versus a monolithic procedure in fluid–structure interaction. *Comput. Struct.*, 87(11-12):793–801, June 2009.

[14] Željko Tuković, Aleksandar Karač, Philip Cardiff, Hrvoje Jasak, and Alojz Ivanković. OpenFOAM finite volume solver for fluid-solid interaction. *Transactions of FAMENA*, 42(3):1–31, October 2018.

[15] André da Luz Moreira. Mesh motion methods in OpenFOAM: Analysis and implementation. Technical report, Chalmers University of Technology, 2023. Open Source CFD Course Project Report.

Author Biography

*Nguyen Vinh-Tan received his BE (2002) in Aerospace Engineering from the Ho Chi Minh City University of Technology and PhD (2007) in Computational Engineering from the National University of Singapore in a joint programme with the Massachusetts Institute of Technology. He is currently a Senior Principal Scientist at the A*STAR's Institue of High Performance Computing, Singapore. His research focuses on developing computational methods for modelling and simulations of complex multiphysics engineering systems, with recent emphasis on translating advanced digital capabilities to support sustainable manufacturing, environment and energy applications.*

*Jason Leong received his BE (2007) and PhD (2013) in Mechanical Engineering from Monash University, Malaysia. He is currently a researcher at A*STAR's Institute of High Performance Computing, Singapore, where his work focuses on computational fluid dynamics, mulciscale and multiphysics simulation, inkjet printing technologies, and urban microclimate modelling. He has contributed to research in fluid–structure interaction, dispersion modelling, and high-performance computing.*

Satoshi Watanabe received his BS in Precision Mechanical Engineering (1996) and ME in Precision Engineering (1998) from Chuo University, Japan. He joined Seiko Instruments Inc. in 1998 and is currently with Seiko Future Creation Inc. He works on CAE across Seiko Group products, primarily focusing on inkjet printheads and watch development, as well as multiphysics problems involving piezoelectric, vibration, and fluid phenomena. He is a member of the Japan Society of Mechanical Engineers (JSME).

Toshimitsu Morooka received Bachelor's and Doctoral degrees in Engineering from Saitama University, Japan, in 1989 and 2004, respectively. In 1989, he joined Seiko Instruments Inc. and developed measurement devices based on superconductivity. In 2012, he joined SII Printek Inc., where he is engaged in the design of inkjet printheads using CAE.